

# Solar X-ray Flare Hazards on the Surface of Mars\*

David S. Smith<sup>†</sup> and John Scalo<sup>‡</sup>

Department of Astronomy, The University of Texas at Austin, Austin, TX  
78712

## Abstract

Putative organisms on the Martian surface would be exposed to potentially high doses of ionizing radiation during strong solar X-ray flares. We extrapolate the observed flare frequency-energy release scaling relation to total X-ray energies much larger than seen so far for the sun, an assumption supported by observations of flares on other solar- and subsolar-mass main sequence stars. Flare spectra are taken as power laws, with the logarithmic slope a parameter based on the observed statistics of the most energetic hard X-ray flare spectra. We calculate the surficial reprocessed spectra using a Monte Carlo code we developed for the transport of X-rays and gamma rays, including photoabsorption and detailed Compton scattering. Biological doses from indirect genome damage are calculated for each parameterized flare spectrum by integration over the X-ray opacity of water. The resulting doses depend sensitively on spectral slope, which varies greatly and unsystematically for solar flares. Using the roughly uniform observed distribution of spectral slopes, we estimate the mean waiting

---

\*To be published in *Planetary and Space Science*.

<sup>†</sup>Corresponding author

<sup>‡</sup>E-mail: {dss,parrot}@astro.as.utexas.edu

time for solar flares producing a given biological dose of ionizing radiation on Mars and compare with lethal dose data for a wide range of terrestrial organisms. These timescales range from decades for significant human health risk to 0.5 Myr for *D. radiodurans* lethality. Such doses require total flare energies of  $10^{33}$ – $10^{38}$  erg, the lower range of which has been observed for other stars. Flares are intermittent bursts, so acute lethality will only occur on the sunward hemisphere during a sufficiently energetic flare, unlike low-dose-rate, extended damage by cosmic rays. We estimate the soil and CO<sub>2</sub> ice columns required to provide  $1/e$  shielding as 4–9 g cm<sup>-2</sup>, depending on flare mean energy and atmospheric column density. Topographic altitude variations give a factor of two variation in dose for a given flare. Life in ice layers that may exist  $\sim 100$  g cm<sup>-2</sup> below the surface would be well protected. Finally, we point out that designing spacesuits to sufficiently block this radiation on Mars missions may be difficult, given the conflict between solutions for lightweight protection from energetic particles and those from X-rays.

## 1 Introduction

Habitability for all types of life—from human to microbial—is a central problem for the next decades of Mars exploration. In particular, knowledge of surficial radiation doses from all possible sources is essential. Cordoba-Jabonero et al. (2003) have calculated in detail the transfer of ultraviolet (UV) radiation in the Martian atmosphere and folded the surface flux with a DNA action spectrum to obtain UV dose rates (see also Cockell et al., 2000, Mancinelli and Klovstad, 2000). Schuerger et al. (2003) treated the same problem experimentally, with the survival of spores of *Bacillus subtilis* in a Mars simulation chamber. Molina-Cuberos et al. (2001), Pavlov et al. (2002), and De Angelis et al. (2004) have estimated the fluxes of Galactic cosmic-ray particles on the present and ancient Martian surface and

subsurface. Pavlov et al. find that the maximum dose rate due to Galactic cosmic rays is about  $0.2 \text{ Gray yr}^{-1}$ , using dosimetry units in which  $1 \text{ Gray (Gy)} \equiv 100 \text{ rad}$  and  $1 \text{ rad} \equiv 100 \text{ erg g}^{-1}$  absorbed. This dose rate occurs at a depth of about  $25 \text{ g cm}^{-2}$ . Measurements and detailed simulations of the cosmic-ray dose rate have been carried out by the Martian Radiative Environment Experiment (MARIE) on the Mars Odyssey Orbiter (see Saganti et al., 2004), with measured and modeled surface values mostly around  $0.06 \text{ Gy yr}^{-1}$ . Integrated over a microorganism's lifetime, the corresponding doses are smaller than the lethal dose for any terrestrial microorganism, but the whole-body human dose would be significant over decades, suggesting problems for manned Mars missions. The dose due to ionizing radiation is also of interest concerning natural transfer of microorganisms between solar system bodies, in particular Mars and Earth (Mileikowsky et al., 2000).

X-rays from the most energetic solar flares are potentially important for Martian habitability, but have not yet been treated. The steady solar coronal X-ray, EUV, and FUV emission is currently fairly small (see Güdel et al., 2003). In contrast, during a solar flare, the flux of ionizing photons can increase by orders of magnitude, and large dose rates are possible. Unlike on Earth, the Martian atmosphere is currently thin enough that a significant fraction of this radiation can arrive at the surface, where it may lead to genetic damage and mutations in terrestrial-like organisms. The fraction of energy absorbed in the atmosphere or reprocessed to UV (see Smith et al., 2004a,b) is minimal. Moreover, the X-ray flux from the flares of interest here are orders of magnitude larger than the Martian keV X-ray fluxes observed by the Chandra X-ray Observatory (Dennerl, 2002) that are probably generated in the Martian atmosphere by solar X-rays (see Cravens and Maurelis, 2001) and the solar wind (see Gunell et al., 2004)

Evolution of enhanced resistance to the X-ray flares discussed in the present work does not seem possible for anything analogous to terrestrial evolution. The flare durations are very short (about an hour), and the times between exposures

are orders of magnitude larger than organism lifetimes, so no adaptation could occur. Thus highly intermittent flare radiation can be lethal in a way that gradually increasing UV (or nearly constant cosmic rays) cannot.

In this paper, we focus on the following question: At the Martian surface, for a strong solar X-ray flare of given total energy and spectrum, how does the biological dose compare to the lethal doses of various terrestrial organisms? We then extrapolate the recurrence frequency-energy release relation for solar flares to estimate the mean time between such lethal events for a variety of organisms. Finally, we contrast X-ray dose rates with that of cosmic rays and discuss shielding considerations.

## 2 Solar Flare Properties

### 2.1 Spectra

X-rays and  $\gamma$ -rays with energies between  $10^{-1}$  and  $10^6$  keV<sup>1</sup> comprise a significant fraction of solar flare photon emission (e.g. Haisch et al., 1991; Hudson, 1991; Kanbach et al., 1993; Ryan, 2000). Hard X-ray (hereafter HXR) spectra are often taken to peak around 10–25 keV (Crosby et al., 1993; but see Krucker and Lin, 2002), but this is very uncertain because it is near the sensitivity cutoff of most pre-RHESSI instruments (see Battaglia et al., 2005). Flare X-ray spectra are often fit by a single power law (Crosby et al., 1993; Bromund et al., 1995; Veronig et al., 2002) or two piecewise power laws (Krucker and Lin, 2002). The range of the estimated power-law spectral index (log-log slope)  $p$  is large for hard X-ray flares (see Lee et al. 1993, Bromund et al. 1995; also Qiu et al. 2004 for HXR microflares): most flares have a  $p$  between 2.5 and 6, with a median around 4 and little correlation with total X-ray output. Using results from RHESSI, Battaglia et al. (2005) find that the non-thermal (hard X-ray) emission spectral index is correlated with total

---

<sup>1</sup>1 Å = 12.4 keV

energy release, such that the larger flares have flatter (harder) spectra. These were relatively low-energy flares, but if a similar relation holds for the most powerful flares, then the large solar X-ray flares described here may deliver even larger doses than we estimate (see §4.2). Given the uncertainty described, we take the slope of the incident photon spectrum as a parameter (see §3), constrained by the observed distribution of  $p$ , and assume no correlation between spectral index and total energy output. As mentioned above, this likely gives a lower limit on the dose estimates.

## 2.2 Durations

Solar flares have a complex temporal structure. The distribution of flare durations has been estimated using several datasets and characteristically fits a decreasing power law (e.g. Lee et al., 1993). Most HXR flares have short durations ( $\lesssim 20$  sec), with a loose correlation between duration and total energy release. We are only concerned with the rare, highest-fluence flares, however, with durations found by Crosby et al. (1993) for HXR and Veronig et al. (2002) for SXR flares of about 15 min, with the more energetic flares tending to last longer. The X-class data of Veronig et al. have a median duration three times longer than the B-class data (30 min and 10 min, respectively). Just as with spectral slope, the flare-to-flare variation in duration is large and difficult to characterize quantitatively. For example, some flares emit much of their energy as gamma rays over several hours (see Ryan, 2000).

For our purposes, though, the duration is unimportant; the acute lethal dose is almost always independent of dose rate (Sparrow et al., 1967), and thus depends on fluence, not flux. Note that almost all flares have durations much smaller than a Martian day, suggesting that mutation and lethality could occur only on one hemisphere at a time. On the other hand, flare events clustered over many days are sometimes observed (e.g., the Halloween flares of Oct–Nov 2003; Woods et al., 2004) that could progressively irradiate the whole planet.

### 2.3 Energy Release

The total photon energy release in flares is difficult to estimate and varies by at least  $10^8$  from flare to flare, but a large number of studies using EUV, soft X-ray (SXR), or hard X-ray (HXR) satellite events roughly agree that the differential distribution of flare energy releases  $dN/dW$  is a power law with index about  $-1.6$  to  $-1.8$  over at least six orders of magnitude in total energy release  $W$  (see Hudson, 1991; Lee et al., 1993; Crosby et al., 1993; Bromund et al., 1995; Aschwanden et al., 2000; Lin et al., 2001; Güdel et al., 2003; Qiu et al., 2004; and references therein), although a somewhat steeper index ( $-2.0$ ) has been inferred from a very large sample of SXR flares (Veronig et al., 2002).

Eleven large X-class flares occurred during the extraordinary solar outbursts between 18 October 2003 and 5 November 2003, with SXR releases in the GOES 1–8 Å ( $\sim 2$ –10 keV) band peaking at about  $2 \times 10^{31}$  erg for an effective duration of 30 min. Observations using the SORCE instrument’s Total Irradiance Monitor yielded a total flare energy at all wavelengths for the somewhat weaker 28 October flare of  $4.6 \times 10^{32}$  erg (Woods et al., 2004). Radiation and charged particles from these flares compressed the Earth’s Van Allen belt to within 20,000 km of the surface (Baker et al., 2004), temporarily damaged the orbiting Mars Odyssey communication instruments, and significantly reduced stratospheric ozone levels (Randall et al., 2005).

Based on astronomical observations, we believe it reasonable to infer that much more energetic solar flares have occurred in the past:

1. There is little doubt that solar-like stars can produce very energetic, and frequent, X-ray flares. Data presented by Audard et al. (2000) indicate SXR flares (0.01–10 keV) of energy greater than  $3$ – $5 \times 10^{34}$  erg for the young, solar-like stars 47 Cas and EK Dra (age  $\sim 100$  Myr) and  $2 \times 10^{33}$  erg for an older, solar-like star  $\kappa$  Cet (age  $\sim 1$  Gyr), with frequencies of about *one per ten days* at these energies. Considering the short sampling period and the form of the derived frequency-

energy release relation, more energetic flares seem likely, though less frequent.

2. Schaefer et al. (2000) have identified nine “superflares” with energy outputs of  $10^{33}$  to  $10^{38}$  erg on otherwise normal F8–G8 main sequence stars. Two of these stars were solar-like and produced X-ray flares with energies about 100–1000 times larger than the largest observed solar X-ray flare. These flares cannot be attributed to binaries, rapid rotation, or youth, and may in fact be common in solar-type stars, although cannibalization of giant planets has been suggested (Rubenstein and Schaefer, 2000).

3. Stothers (1980) interpreted  $\text{NO}_3^-$  abundance spikes in several Antarctic ice cores as due to flares with energies around  $10^{32}$ – $10^{33}$  erg with a recurrence timescale of  $\sim 10^2$  yr, consistent with the extrapolation of the frequency-energy relation we adopt below in Eq. 6.

4. On lower mass dMe main-sequence stars, flares are more frequent, with photon releases exceeding  $10^{34}$ – $10^{35}$  erg observed, often serendipitously (Hawley and Pettersen, 1991; Pagano et al., 1997; Liebert et al., 1999; Favata et al., 2000; Christian et al., 2003). These energies are enormous, considering that the bolometric luminosities of these stars are much smaller than that of the sun.

Although flares of such large energy release have not been observed in the sun, these data for other stars strongly suggest that the maximum observed is limited only by duration of observation. We have found no compelling physical argument for an upper limit to flare energy releases below the levels discussed in this paper, but the slope of the empirical frequency-energy release relation suggests that some upper limit must exist to avoid energy divergence (Hudson, 1991). Limits on energetic *particle* fluxes (e.g., Lingenfelter and Hudson, 1980) are due to self-confinement effects and cannot be applied to photons. Given the above considerations, we expect the the maximum flare release to be *at least*  $10^{34}$  erg and assume this to be true in what follows.

### 3 Radiative Transfer Method

We calculate in detail the transfer of the incident ionizing radiation through the Martian atmosphere using a previously developed Monte Carlo code (Smith et al., 2004b) that accurately treats Compton scattering and X-ray photoabsorption. We use the empirical approximation of Setlow and Pollard (1962) for the photoabsorption cross section for energies greater than the K edge:

$$\sigma_{\text{pa}} = 2.04 \times 10^{-30} (1 + 0.008Z) \left(\frac{Z}{E}\right)^3 \text{ cm}^2, \quad (1)$$

where  $E$  is the energy in units of 511 keV and  $Z$  is the atomic number of the target atom. We have compared this with the NIST database of cross sections and find good agreement. Compton scattering cross sections are calculated using the full Klein-Nishina formula. We assume that the atmospheric gas density falls off exponentially with height, with a scale height of 11 km and a total column density of 16 or 22 g cm<sup>-2</sup>, corresponding to rough limits set by the freezing and thawing of the polar ice caps. This model works well because the high-energy radiative processes involved here are relatively insensitive to the exact vertical distribution and composition of gas, instead depending mainly on the total column density and mean molecular weight.

Solar flare photon number spectra are assumed to be distributed as  $E^{-p}$ , with  $2 \leq p \leq 6$  (see §2). For calculational purposes, the flare spectrum is assumed to extend from 10 keV to 511 keV. The 10-keV lower limit is taken because photons below this energy are nearly completely absorbed by the atmosphere and unimportant to the surficial dose, while the upper limit is set high enough that a negligible number of incident photons are at higher energies, even for the shallowest spectra (lowest  $p$ ). Given a lower limit  $E_{\text{min}}$  and a specified normalization  $N_{\text{tot}}$ , the differential number spectrum can be written (neglecting any upper cutoff for simplicity)

$$\frac{dN}{dE} = (p-1) N_{\text{tot}} E_{\text{min}}^{p-1} E^{-p}, \quad (2)$$

and the average energy in the spectrum is obtained by integrating between the minimum and maximum cutoff energies:

$$\langle E \rangle = \frac{1}{N_{\text{tot}}} \int_{E_{\text{min}}}^{E_{\text{max}}} E \frac{dN}{dE} dE. \quad (3)$$

This is the spectrum that is propagated through the atmosphere using the Monte Carlo code. Note that henceforth the total energy release figures refer only to the energy between 10 and 511 keV.

After transport through the atmosphere, the photon fluence is converted to a biological dose by assuming that the surficial radiation is absorbed by pure water. Much of the damage by ionizing radiation is thought to be “indirect,” involving chemical reactions initiated by energy deposited in the bulk cell water or first hydration layer rather than “direct” ionization of DNA (von Sonntag, 1987; see Ward, 1999, and references therein), although this terminology is now recognized as an oversimplification (see Fielden and O’Neill, 1991). We then estimate the dose by integrating the surficial energy spectrum  $E dN/dE$  over the energy-dependent opacity of water  $\kappa_w(E)$ :

$$D = \int_{E_{\text{min}}}^{E_{\text{max}}} \kappa_w(E) E \frac{dN}{dE} dE. \quad (4)$$

The water opacity in our code includes both Compton scattering and photoabsorption. It should also be noted that the biological quality factor and relative biological effectiveness (RBE) are both near unity for X-rays and  $\gamma$ -rays, so no adjustment is required to compare to empirical lethal doses, as in cosmic-ray studies.

Most of the uncertainty in our calculations is due to the fact that the total X-ray opacity of the Martian atmosphere depends sensitively on the uncertain energy spectrum of the flare photons, since the photoabsorption optical depth varies approximately as  $\exp(-E^{-3})$ . Given a particular flare spectrum, our results are accurate, but the spectral slopes vary greatly from flare to flare, even given the same total energy release (see §2). Thus we use the slope,  $p$ , as a free parameter that varies between 2 and 6 and present the results for a range in  $p$ . Later we integrate

over an approximate representation of the observed frequency distribution of  $p$  for hard X-ray solar flares to derive appropriate average values for waiting times as a function of dose.

## 4 Results

### 4.1 Calculated Surficial X-Ray Spectra

The Martian atmosphere, though thin by terrestrial standards, significantly attenuates the incident flare radiation, but the high fluences associated with the most massive flares lead to extreme irradiation of the surface nonetheless. We show in Fig. 1 the surficial fluence spectra from a  $10^{35}$  erg flare for two atmospheric column densities ( $\Sigma = 16$  and  $\Sigma = 22$  g cm<sup>-2</sup>) and two spectral indices ( $p = 4$  and  $p = 2.5$ ), together with the above-atmosphere, incident spectra. The vertical axis scales linearly with flare energy release (we have used  $10^{35}$  erg for this example). In general, for all column densities, spectra with lower mean energies (higher  $p$ ) are attenuated more because of the rapidly rising ( $E^{-3}$ ) photoabsorption opacity. This effect, combined with the falloff of the incident spectrum at high energies, together creates a peak in the surficial spectrum at moderate energies (30–50 keV here). Additionally, increasing the atmospheric column increases the attenuation at all energies, as one would expect.

### 4.2 Estimated Biological Doses

Ionizing radiation alters DNA through direct ionization and indirect chemical interactions involving diffusion of radical products of ionization and dissociation in the cytoplasm. Resulting biochemical effects include single- and double-strand breaks, base damage or abasic sites, multiply damaged sites, oxidized base clusters, and cross-linking within DNA or with proteins (see Becker and Sevilla, 1993; Ward, 1999). An amazing suite of repair processes and associated enzymes repair the

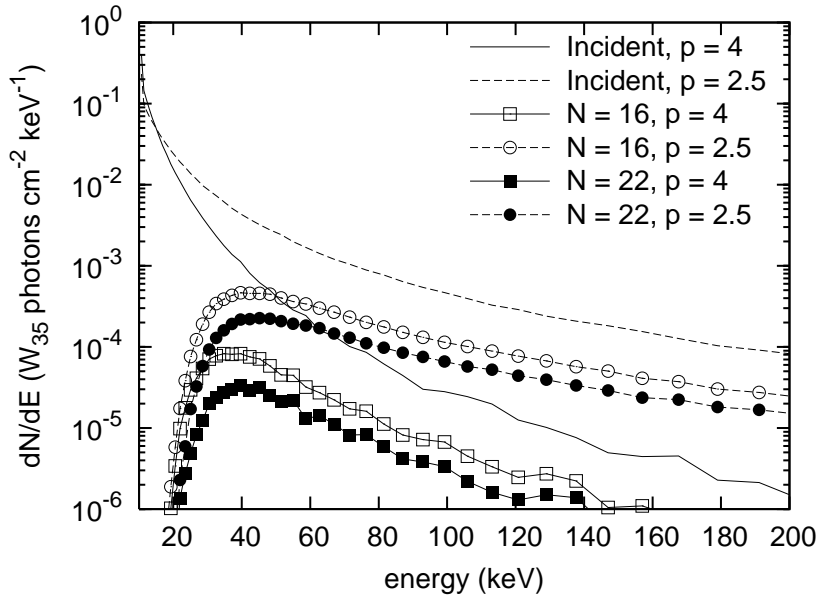


Figure 1: Surficial, reprocessed, X-ray flare spectra, assuming a parameterized, power-law model spectrum (see §3). Two incident spectra are shown, with power-law spectral indices of  $p = 2.5$  and  $p = 4$ . For each of these spectra, associated surficial spectra are shown for two different column densities: 16 and 22  $\text{g cm}^{-2}$ . Attenuation due to photoabsorption is most severe at low energies, leading to a sharp decline below about 20 keV in the flux per unit energy. Also, the original incident spectrum falls off at high energy, so the combined effect leads to a peak at intermediate energies (30–50 keV here).

damage (Friedberg, 2003, and references therein), but generally for each organism, above some critical amount of absorbed energy, fecundity greatly diminishes. Biological damage is quantified in terms of the amount of energy absorbed, or dose, typically in units of rads or Grays (1 rad  $\equiv$  100 erg g<sup>-1</sup> absorbed; 1 Gray  $\equiv$  100 rad). The lethal dose is often defined as the dose that kills a particular fraction of a laboratory population. The dose for reducing the population by  $1/e$  is denoted  $D_{37}$ , while the dose for reduction of the population by 90% is  $D_{90}$ .

The calculated X-ray doses in our situation are shown in Fig. 2 as a function of power-law index for two column densities:  $\Sigma = 16$  g cm<sup>-2</sup> and  $\Sigma = 22$  g cm<sup>-2</sup>. The calculation assumes a solar flare with a total X-ray release of  $10^{35}$  erg (see §2). Again, for flares of different energy release, the dose simply scales proportionally. The doses for the shallowest spectra ( $2 \leq p \leq 3$ ) are about two orders of magnitude higher than those for the steepest spectra ( $5 \leq p \leq 6$ ), showing the tremendous sensitivity of the dose on the form of the incident spectrum. For comparison to the power-law spectra, we also show monoenergetic spectra with energies equal to the average energy in the power-law spectra for each spectral index. The dramatic decline in the dose with energy for the monoenergetic cases illustrates the importance of the high-energy tail in the power-law spectra and the inaccuracy of doing this calculation using a monoenergetic approximation.

The results shown in Fig. 2 can be confirmed by considering a  $10^{35}$ -erg flare incident on the top of the atmosphere and subject to only absorption due to Compton scattering and photoabsorption. Strictly speaking, the Compton process is a scattering process, not absorption, but we will neglect photons that backscatter in the atmosphere and eventually reach the surface in order to get this estimate. This enables us to write an integral that approximates the total dose  $D$  in terms of the atmospheric optical depth  $\tau_a(E)$  and the water opacity  $\kappa_w(E)$ :

$$D = \int_{E_{\min}}^{E_{\max}} \kappa_w(E) \exp[-\tau_a(E)] E \frac{dN}{dE} dE, \quad (5)$$

where  $N(E)$  is the incident number spectrum at the top of the atmosphere and  $E_{\min}$

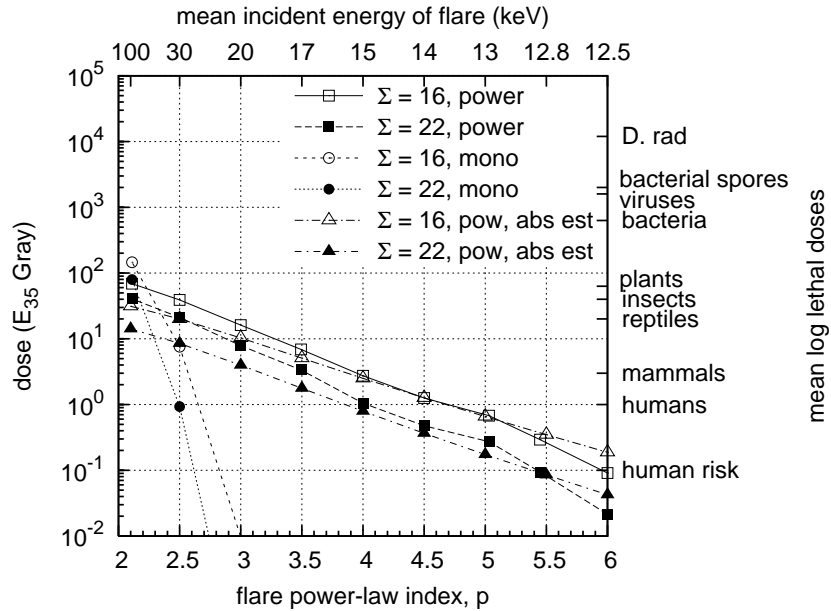


Figure 2: Surficial X-ray dose for a flare with  $10^{35}$  erg total energy release versus spectral index. (Doses scale linearly with energy release.) Two column densities are used: 16 and 22  $\text{g cm}^{-2}$ . Power-law flare spectra are denoted “power” in the legend. Monoenergetic incoming photons with energies equal to the mean incident flare energy are shown as “mono.” This case demonstrates the inaccuracy of ignoring the full radiative transfer, since the curve decreases *much* more rapidly than the power-law cases. The final pair of curves (denoted “abs est”) uses a power-law incident spectrum with the radiative transfer done using the analytic, absorption approximation discussed in §4.2. The general trend among all curves is that the dose decreases with increasing spectral index. This is because (as can be seen on the upper horizontal axis) the average energy of the flare spectrum decreases with increasing spectral index. The atmosphere is vastly more opaque to lower-energy X-rays, which dramatically affects the surficial dose. The right-hand vertical axis shows tick marks at the mean-log lethal dose of a few representative terrestrial organisms (see Table 1).

is the minimum energy considered in the Monte Carlo code. This integral can be evaluated numerically to confirm the results given in our Monte Carlo calculation; we have done this and present it as the final set of curves in Fig. 2 marked “abs est.” The integral is very close to the full calculation at all energies, being only different by at most a factor of two, which suggests that backscattered radiation is only marginally important to the surficial doses. For the flattest spectra ( $p$  near 2), the code gives a higher (and more accurate) dose because it includes backscattered radiation. For steeper spectra, the difference between the above approximation and the code stems from the discrete number of bins in the surficial spectra in the code and the fact that the mean incident spectrum energy is very close to the lower cutoff energy, causing discretization errors in the output spectra when binning photon energies close to the cutoff. The integral above, being continuous, suffers no such errors, so is probably more accurate in this regime, where absorption dominates anyway.

The horizontal ticks along the right side of Fig. 2 show typical mean-log acute lethal doses for a variety of organisms. The most comprehensive compilation we know of, Sparrow et al. (1967), gives  $D_{90}$  for X-ray and  $\gamma$ -ray exposure of 79 organisms. We have expanded and supplemented this with more recent work, especially for microorganisms, including the review of virus lethal doses by Rohwer (1984), lethal doses in bacterial spores summarized by Russell (1982), studies of food pathogenic bacteria by Dion et al. (1994) and Farkas (1998), studies of Archaean hyperthermophiles by Kopylov et al. (1993) and DiRuggiero et al. (1997), mammalian studies presented in Fielden and O’Neill (1991), studies of mutations in human survivors of Hiroshima and Nagasaki (see Turner, 1995, p. 398), the Chernobyl accident and Kazakhstan nuclear weapon tests (Dubrova, 2003), and inhabitants of the Kerala (India) radioactive hotspot (Forster et al., 2002). We find these results to be consistent with each other in cases we have checked.

Table 1: Acute lethal dose ranges for representative organisms

Organism	Acute Lethal Dose (Gy)
mammals	1–10
higher plants	5–700
insects	1–2000
bacteria, protozoa, algae	30–15,000
viruses	150–20,000
bacterial spores	1,000–4,000

Because of the large range of lethal doses found in nature we have chosen to represent various organisms in Fig. 2 by the average of the base-10 logarithm of the lower and upper limits found for that class. This is an appropriate choice because the available data from Sparrow et al. (1967) within each taxonomic class are distributed roughly uniformly in log lethal dose. Thus for mammals, with a range of 1–10 Gy, the number indicated on the log scale is 0.5. Table 1 lists the approximate lethal dose ranges for these organisms. Organisms with extremely large lethal doses are interesting for long-term survival prospects—e.g. adult *Drosophila* at 1000 Gy, some Archaean hyperthermophiles at 2000–6000 Gy, *Rubrobacter radiotolerans* at 8000 Gy (Ferriera et al., 1999), *Deinococcus radiodurans* at 10,000 Gy (depending on cell phase; see Battista, 1997), and the virus-like proteinaceous infectious particle (prion) associated with scrapie at 20,000 Gy (Rohwer, 1984).

Even very low doses can be important. Doses for mutation and clustered DNA damage can be much smaller than the lethal dose. For example, in humans, the whole-body acute lethal dose is about 1–2 Gy, but mutations (Sparrow et al., 1972; Sankaranarayanan, 1982; Forster et al., 2002), chromosomal abnormalities in blood lymphocytes (Violot et al., 2005), and clustered DNA damage (Sutherland et al., 2000) occur at only around 0.01–0.2 Gy, and germ-line mutation doubling is believed to occur around 0.5 Gy (UNSCEAR 2001; Sankaranarayanan and

Chakraborty, 2000; but see Forster et al., 2002). So doses even smaller than the “humans” level in Fig. 2 should be considered hazardous for human exploration of Mars. We indicate this level at 0.1 Gy with the label “human risk” and emphasize that this value is illustrative, not definitive.

We have ignored the dependence of lethal dose on dose rate. Sparrow et al. (1967) claim no evidence for a significant dependence in the literature they compiled, but it is undoubtedly true that at some level a dose rate dependence occurs, as has been observed in mammalian and other organisms. And since the duration of solar flares is random, it is difficult to convert received fluences into fluxes, which are needed for dose rate calculations, hence we have ignored this and focused entirely on time-integrated quantities in this work.

Finally, recall the possible correlation between hard X-ray flux and spectral index found in the RHESSI data by Battaglia et al. (2005) mentioned in §2.1. If flares with a larger total energy release do indeed typically have flatter spectra, then they would have higher mean photon energies. The Martian atmosphere is more transparent to X-rays of higher energies, so this effect would boost the surficial doses received from larger flares. So in this sense our results are an upper limit to the flare releases required to produce given doses.

### 4.3 Mean Times Between Lethal Events

The calculated surficial doses are very sensitive to the flare spectral index  $p$ , which varies greatly and unsystematically with other flare parameters, so a better way to determine the lethality risk is to integrate the frequency of events delivering a given dose for each  $p$  over the probability distribution of  $p$  values. We take this probability distribution to be the uniform distribution, which is roughly consistent with results shown in Lee et al. (1993), Bromund et al. (1995), Veronig et al. (2002), and Qiu et al. (2004) and other references given there. This procedure yields the total frequency of lethal events for an organism at the Martian surface

due to all flares.

To estimate flare timescales as a function of release  $W$ , we normalize to one  $10^{32}$ -erg solar flare per decade. Extrapolating the average HXR frequency-energy statistic  $dN/dW$  (see §2) gives the average time between events of energy release  $W_{32}$  (in units of  $10^{32}$  erg) as  $T(W) \simeq 10W_{32}^q$  yr, with  $q$  between about 1.6 and 1.8, and the mean time between events at least as large as  $W_{32}$  as

$$T(\geq W_{32}) = 10(q-1)W_{32}^{q-1}\text{yr}. \quad (6)$$

This agrees with the estimate of Hudson (1991) and is broadly consistent with the dozen or so  $10^{31}$ – $10^{32}$  erg events that have been observed since GOES soft X-ray monitoring began in 1976. Upper limits on proton fluences in lunar rocks, tree ring records of  $^{14}\text{C}$ , and the requirement of finite energy suggest that the frequency-energy release relation  $dN/dW$  must steepen above some energy (Reedy et al., 1983; Hudson, 1991; Aschwanden, 1999), but the value of that energy is unknown.

Figure 3 graphically shows the mean time between lethal events for the same set of organisms given in Fig. 2 as a function of surficial dose, for an atmospheric column density  $\Sigma$  of  $16 \text{ g cm}^{-2}$ . To produce this plot, we use the mean of the empirical values of frequency-energy release slope, so  $q = 1.7$  in Eq. 6. The right-hand side vertical axis shows the corresponding flare energy releases  $W$  required for lethality. Again, this result is integrated over the spectral index distribution. Additionally, for a column density of  $22 \text{ g cm}^{-2}$ , the attenuation is roughly a factor of 2–3 higher (as can be see in Fig. 2), so the required lethal dose would be roughly a factor of 2–3 higher, implying a mean waiting time that is  $2^{0.7}$ – $3^{0.7} = 1.6$ – $2.2$  times longer.

The mean time to lethality is strongly weighted toward the flattest ( $p \sim 2$ ) flares. The atmosphere is more transparent to the flatter flares (because they have a higher average energy), so a lethal fluence at the surface requires less total energy release at the sun. Since flares with lower total energy release are much more common, chances are that the flare that finally delivers the lethal dose will have a

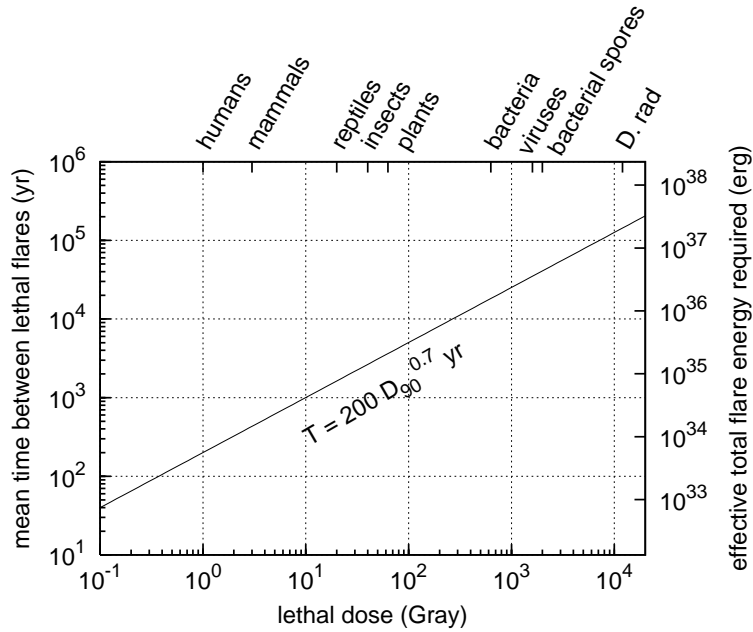


Figure 3: Mean time between flare events that deliver a given dose. The dose delivered depends on the spectral index, such that flares with larger spectral index must have a larger total energy to deliver a given dose (see Fig. 2). We have integrated over the distribution of spectral indices, and accounted for the dose dependence on this index, in order to find a mean time between events that deliver a given dose without specifying the spectral index (see §4.3). The upper horizontal axis shows the lethal doses of a variety of organisms for reference (see Table 1). As expected, the time between events increases as the dose necessary for lethality increases.

smaller spectral index. We show this explicitly below.

To derive the equation for the mean time between flares of a given dose, as shown in Fig. 3, we first convert the waiting time distribution given in Eq. 6 back to the empirical flare energy release-mean frequency relation:

$$\bar{v}(W) = k_W W_{32}^{-q} \text{ yr}^{-1}, \quad (7)$$

where once again we use  $q = 1.7$  and we estimate  $k_W \sim 0.1$ . The flares are roughly distributed uniformly by spectral index  $p$ , and since  $p$  ranges from 2 to 6, we can write the probability distribution function of  $p$  as  $f(p) = 1/4$ . The frequency distribution for the flares as a function of energy  $W$  and spectral index  $p$  is then

$$\bar{v}(W, p) = \bar{v}(W) f(p), \quad (8)$$

where we have assumed that  $W$  and  $p$  are uncorrelated.

To predict how often solar X-ray flares can deliver a particular lethal dose, we must transform this distribution to a function of dose  $D$ . This requires knowledge of the relation between total flare energy release and surficial dose for each spectral index  $p$ . In our case, this relation comes from our radiation transport code. An empirical fit to our calculations for a column density of  $16 \text{ g cm}^{-2}$  shows that the dose in Gray as a function of flare energy is

$$D(W, p) = \frac{W_{32}}{k_D} e^{-p/p_0} \text{ Gy}, \quad (9)$$

with  $k_D = 0.23$  and  $p_0 = 0.53$ . We can write the energy required to deliver a given dose by inverting this equation. Then, using the standard technique for transforming probability distribution functions, we have

$$\bar{v}(D, p) = \bar{v}[W(D, p), p] \left| \frac{\partial(W, p)}{\partial(D, p)} \right| \quad (10)$$

$$= \bar{v}[W(D, p)] \left| \frac{dW}{dD} \right| f(p) \quad (11)$$

$$= \frac{k_W k_D^{1-q}}{4} D^{-q} \exp[(1-q)p/p_0] \text{ yr}^{-1}. \quad (12)$$

Next, we would like to know how many flares of all spectral indices occur each year, but now the dose and spectral index are not independent, so we must integrate, instead of just scaling by 1/4:

$$\bar{v}(D) = \int_2^6 \bar{v}(D, p) dp \quad (13)$$

$$= \frac{k_W k_D^{1-q} p_0}{4(q-1)} D^{-q} \{ \exp[2(1-q)/p_0] - \exp[6(1-q)/p_0] \} \text{ yr}^{-1}. \quad (14)$$

All flares that deliver doses above the lethal dose are most definitely lethal, so we must integrate the flare dose-mean frequency distribution above the lethal dose (we use  $D_{90}$  here) to find the total number of flares that occur on average per year that deliver at least the lethal dose:

$$\bar{v}(\geq D_{90}) = \int_{D_{90}}^{\infty} \bar{v}(D) dD \quad (15)$$

$$= \frac{k_W k_D^{1-q} p_0}{4(q-1)^2} \{ \exp[2(1-q)/p_0] - \exp[6(1-q)/p_0] \} D_{90}^{1-q} \text{ yr}^{-1}. \quad (16)$$

Finally, to get the mean time between lethal events, simply take the inverse of this frequency:  $\bar{T}(\geq D_{90}) = 1/\bar{v}(\geq D_{90})$ . For the case discussed in this work,  $k_W \sim 0.1$  and  $q = 1.7$ . Thus the typical time between lethal flares as a function of lethal dose in Gray is

$$\bar{T}(\geq D_{90}) \simeq 200 D_{90}^{0.7} \text{ yr}. \quad (17)$$

This time is much shorter than an estimate using just a particular  $p$  value yields. For example, using  $p = 4$  instead of integrating over the distribution of  $p$  would give about 3000 yr for the coefficient above instead of 200 yr. Properly treating the spectral indices as a distribution in the calculation is important, rather than just assuming that  $p = 4$  is the representative index and making simple estimates based on that. In fact, the true waiting times are probably a bit shorter than our estimate, since the distribution of spectral indices isn't exactly flat, but rather is peaked slightly at lower indices. In other words, the average flare spectrum may be somewhat harder than we take here.

Figure 3 indicates that a solar X-ray flare of  $10^{38}$  erg would be needed to kill any organism as resistant as *D. rad*, bacterial spores, and the most resistant viruses (see Table 1) on the surface of Mars. Such flares would occur at least every  $\sim 200$  kyr if our extrapolation of the solar frequency-energy release scaling could be extended to these extreme energies. Since such energies have not been observed in the sun or other (non-binary) stars, we conclude that such extremely radiation-resistant microbial life on Mars may not be affected by solar flares. Bacteria and protists with the adopted mean log lethal dose require slightly less extreme flare energies and have corresponding times to lethality of about 20 kyr. Reptiles, insects, and plants require more reasonable flare energies, especially considering that many have lethal doses much less than the mean log (see Table 1 and Sparrow et al., 1967). Flares of only  $10^{34}$ – $10^{35}$  erg will result in mutations and lethality for mammals, reptiles, insects, and plants, and may occur every few hundred years. Similarly, a  $10^{34}$ -erg flare, which can be lethal to humans, might occur every 200 yr on average. We conclude that no organisms other than the most resistant bacteria and viruses could have survived on the surface of Mars during the past  $\sim 10^5$  yr, which is almost certainly much smaller than the time during which Mars has had its current low-column-density atmosphere.

Additionally, a correlation between hard X-ray flux and total flare energy release in which larger flares have harder (flatter) spectra (e.g., Battaglia et al., 2005) would decrease the time between lethal events. Larger flares would be more penetrating and would deliver higher doses than we have estimated, which would decrease the energy release needed for a given dose. Since less energetic flares are more common, lethality would occur more often.

## 4.4 Shielding and Dose Rate Considerations

### 4.4.1 Soil and CO<sub>2</sub> Ice Shielding

So far, we have ignored possible protection strategies, such as radiation shielding sources. As an illustrative example, we take the Mars Pathfinder rover soil sample data of Wänke et al. (2001) and calculate the opacity of this material to incoming flare spectra. Based on the composition of the soils in Table I of Wänke et al. (2001), we find that the samples have an effective atomic number of 15.2 (the  $Z$  that, when used in Eq. 1, yields the mean cross section of the soil obtained by element-by-element addition). The combined photoabsorption and Compton scattering opacity of this material can be calculated. We use the analytical approximation in Eq. 5 to calculate the transfer of the surficial radiation through the soil. Using an atmospheric column density of  $16 \text{ g cm}^{-2}$ , we find  $1/e$  (i.e., optical depth unity) shielding columns for X-ray flares of spectral index  $p = 2$  and  $p = 6$  to be  $7.7 \text{ g cm}^{-2}$  and  $3.6 \text{ g cm}^{-2}$ , respectively. For an atmospheric column density of  $22 \text{ g cm}^{-2}$ , the same calculation gives only a slightly different result:  $8.1 \text{ g cm}^{-2}$  and  $3.9 \text{ g cm}^{-2}$ , respectively. With a typical density of terrestrial andesites of  $2.7 \text{ g cm}^{-3}$ , these soil columns suggest that around a few cm of regolith is enough to provide  $1/e$  attenuation and that tens of cm will reduce the dose by 99% or more. For comparison, the possible ice layers found by Boynton et al. (2002) at 40–150  $\text{g cm}^{-2}$  below the surface should be very well shielded.

CO<sub>2</sub> ice has an effective  $Z$  of 7.4, roughly half that of the soil, so  $1/e$  shielding requires a slightly larger ice column. For an atmospheric column density of  $16 \text{ g cm}^{-2}$ , we find  $1/e$  shielding columns of CO<sub>2</sub> ice for spectral indices  $p = 2$  and  $p = 6$  to be  $8.2 \text{ g cm}^{-2}$  and  $4.6 \text{ g cm}^{-2}$ , respectively. For a column density of  $22 \text{ g cm}^{-2}$ , we get  $8.6 \text{ g cm}^{-2}$  and  $4.9 \text{ g cm}^{-2}$ , respectively. Roughly three times the thickness of ice would be needed for the same  $1/e$  shielding as corresponding soil columns due to the different densities. The difference is smaller than expected from the  $Z^3$  dependence of the photoabsorption cross section because a large fraction of

photons in the surficial spectrum, even for steep flare spectra, has energies high enough that the radiative transfer is dominated by Compton scattering, a process insensitive to elemental composition.

Altitude can change the atmospheric column density and have a measurable effect on the dose. The column density above Hellas Basin, the lowest topographical point on Mars, is roughly 8 to 14 g cm<sup>-2</sup> larger (depending on season) than the average and consequently reduces the dose to a factor of about 1/7 to 1/3 of the dose at the mean surface level. This suggests that organisms in low areas would be better protected, but not completely safe. Hellas Basin is an extreme example, and more generally we expect topographic altitude variations to give less than a factor of two variation in dose for a given flare.

#### **4.4.2 Manned Mission Shielding**

Astronaut protection is a critical issue for long-term, manned space missions. The total mass of a spacesuit depends mostly on the column density of the component material, so, given a fixed shielding requirement, the suit's mass will be minimized by maximizing the suit's opacity to incoming radiation. Typical next generation spacesuit designs provide only up to a few g cm<sup>-2</sup> of mostly low-*Z* shielding material (see Ross et al., 1997, for a review). The lightweight and mostly low-*Z* suits are designed to provide efficient protection from incoming energetic particle radiation (such as cosmic rays). Charged particles lose more energy per unit column density traversed in materials with lower *Z* because the energy loss is roughly proportional to *Z/A*, where *A* is the mean atomic mass, and lighter elements maximize *Z/A*. Additionally, low-*Z* materials produce less secondary radiation (mostly neutrons) and lower absorbed doses when incident particles cause nuclear reactions in the shielding material (see, e.g., Schimmerling et al., 1996, and Wilson et al., 2001).

X-ray radiation is most efficiently stopped by high-*Z* materials. Neglecting engineering considerations and particle radiation, the ideal shielding material for

X-rays would maximize the quantity  $Z^3/A$ , because the photoabsorption opacity, which dominates at these energies, has roughly this dependence on  $Z$  and  $A$ , as can be seen in Eq. 1. Thus, heavier elements are favored for X-ray shielding, since atomic mass  $A$  increases much slower than  $Z^3$  across the periodic table. Spacecraft and surface structures, such as “Marsbases,” would probably contain a significant amount of high- $Z$  material, and thus could provide adequate flare X-ray shielding if surrounding structures provide a shielding column of greater than tens of  $\text{g cm}^{-2}$  of  $Z \gtrsim 10$  material. For example, polymers, water, and lower- $Z$  metals, such as magnesium and aluminum, would be less desirable than titanium or steel alloys (especially those high in molybdenum). And even a few  $\text{g cm}^{-2}$  of high- $Z$  material is inadequate should a large solar X-ray flare occur during a spacewalk or “Marswalk.” Balancing the two contrasting shielding requirements for particles and photons while minimizing the weight and rigidity of spacesuits may prove to be difficult.

All of these considerations also apply to moon missions and space missions elsewhere in the solar system, with doses being even higher outside of Mars’ protective atmosphere and inversely proportional to the square of the distance to the sun.

#### 4.4.3 X-ray Flares and Cosmic Rays: Dose Rate Differences

The mean times to lethality we give refer only to the surface of Mars on the hemisphere facing the sun for organisms with short generation times. Lethality from a solar flare contrasts with the situation for cosmic-ray exposure; the difference is one of acute versus extended weak exposure. Flares are intermittent bursts, and lethality will occur during the flare if the flare is sufficiently energetic. The organism lifetime does not affect lethality unless it is less than the mean flare duration (about 10–60 min for the flares considered here), and even most bacteria have longer generation times. For example, the average generation time for many *E. coli*

strains is about an hour. Cosmic rays, however, cause damage over long periods of time from constant, relatively small, surficial fluxes. Organisms might be able to continuously repair the cosmic-ray damage (as on the present Earth), while the high dose rates of flare exposure may overwhelm genomic repair systems. The Saganti et al. (2004) and Pavlov et al. (2002) calculations cited in §1 give Galactic cosmic-ray dose rates of 0.06–0.2 Gy yr<sup>-1</sup>. Taking the representative dose rate to be 0.1 Gy yr<sup>-1</sup>, the time to accumulate a lethal dose from cosmic rays is longer than the lifetime of all but the most sensitive mammals and long-lived plants.

Pavlov et al. (2002) also suggest that living organisms would survive cosmic-ray irradiation because of their short lifetimes, and only dormant organisms, such as spores, with their inactive genomic repair systems, would be killed by the slowly accumulating damage. In contrast, solar flares with very high energies have dose rates high enough to kill living organisms (because the dose is so acute) and possibly contribute to or even dominate the death of dormant organisms. Dormant organisms have radiation tolerances generally much larger than active organisms, but they accumulate damage over a much longer time period. In this case the total dose would be due to a steady dose rate of cosmic rays plus the accumulated acute doses of a large number of individual X-ray flares over the period of dormancy.

## 5 Summary and Implications

Continuing astronomical observational programs are recording larger and larger X-ray flares from stars of solar mass and smaller. The most energetic flares observed on the sun are almost large enough to cause mutation and lethality in higher organisms on the surface of Mars, and extrapolation to higher energies implies greater, but less frequent, biological damage.

Using a previously developed Monte Carlo radiative transport code (Smith et al., 2004b), we have calculated the surficial X-ray spectra and corresponding biological doses due to solar flares with a range of spectral indices. We compared

our results to the average lethal doses for a representative range of terrestrial organisms. We find that, if the sun has flares much larger in energy output than those observed (as supported by observations of other stars), organisms with a range of radiological tolerances, from mammals to plants, insects, and reptiles to even high-tolerance bacteria, spores, and viruses could be killed on the hemisphere of Mars facing the sun during the flare. Though a single flare leads to only partial irradiation, flares are often clustered in time, so it may be possible to irradiate the whole surface over the course of weeks during a period of extreme solar activity.

Estimates were given for the mean time between lethal events based on extrapolating the observed recurrence frequency-energy release distribution for solar flares. Precise results are difficult because of the random nature of flare occurrence and spectral indices, so we provide mean times between lethal flare events integrated over the spectral index distribution. In addition, the estimated mean times between flares of such energies are orders of magnitude less than the age of the solar system, so may have occurred  $10^3$ – $10^7$  times for the period during which Mars has had its present thin atmosphere, depending on the maximum possible solar flare energy and required lethal dose.

Finally, we showed that a column thickness of  $\sim 4$ – $8 \text{ g cm}^{-2}$  of Martian soil would be sufficient to provide  $1/e$  attenuation of the surficial flare energy. The conflicting shielding requirements for particle radiation and the X-rays discussed here leads to a difficulty designing safe spacesuits for manned Mars or lunar exploration, but designing safe “Marsbases” and other ground structures should be easier.

## Acknowledgements

DSS was supported by the NSF Graduate Student Research Fellowship and Harrington Doctoral Fellowship Programs. JMS was supported by the NASA Exobiology Program, Grant NNG04GK43G. This work was carried out as part of the

research of the NASA Astrobiology Institute Virtual Planetary Laboratory Lead Team, which is supported through the NASA Astrobiology Institute.

## References

- Aschwanden, M.J., 1999. Nonthermal flare emission. In: Strong, K.T., Saba, J.L.R., Haisch, B.M., Schmelz, J.T. (Eds.), *The Many Faces of the Sun*. Springer, NY. 273–300.
- Aschwanden, M.J., Tarbell, T.D., Nightingale, R.W., and 5 others, 2000. Time variability of the “quiet” Sun observed with TRACE. II. Physical parameters, temperature evolution, and energetics of extreme-ultraviolet nanoflares. *Astrophys. J.* 535, 1047–1065.
- Audard, M., Güdel, M., Drake, J.J., Kashyap, V.L. 2000. Extreme-ultraviolet flare activity in late-type stars. *Astrophys. J.* 541, 396–409.
- Baker, D.N., Kanekal, S.G., Li, X., Monk, S.P., Goldstein, J., Burch, J.L., 2004. An extreme distortion of the Van Allen belt arising from the “Halloween” solar storm in 2003. *Nature*. 432, 878–881.
- Battaglia, M., Grigis, P.C., Benz, A.O., 2005. Size dependence of solar X-ray flare properties. *Astr. Astrophys.*, in press (<http://arxiv.org/astro-ph/0505154>).
- Battista, J.R., 1997. Against all odds: the survival strategies of *Deinococcus radiodurans*. *Ann. Rev. Microbiology*. 51, 203–224.
- Becker, D., Sevilla, M.D., 1993. The chemical consequences of radiation damage to DNA. *Adv. Radiation Biol.* 17, 121–180.
- Boynton, W.V., Feldman, W.C., Squyres, S.W., and 22 others, 2002. Distribution of hydrogen in the near surface of Mars: Evidence for subsurface ice deposits. *Science*. 297, 81–85.
- Bromund, K.R., McTiernan, J.M., and Kane, S.R., 1995. Statistical studies of ISEE 3/ICE observations of impulsive hard x-ray solar flares. *Astrophys. J.* 455, 733–745.

- Christian, D. J., Mathioudakis, M., Jevremovic, Dupuis, J., Vennes, S., Kawka, A., 2003. The extreme-ultraviolet continuum of a strong stellar flare. *Astrophys. J. Lett.* 593, L105–L108.
- Cockell, C.S., Catling, D.C., Davis, W.L., Snook, K., Kepner, R.L., Lee, P., and McKay, C.P., 2000. The ultraviolet environment of Mars: Biological implications past, present, and future. *Icarus*. 146, 343–359.
- Cordoba-Jabonero, C., Lara, L.M., Mancho, A.M., Márquez, A., Rodrigo, R., 2003. Solar ultraviolet transfer in the Martian atmosphere: Biological and geological implications. *Plan. Sp. Sci.* 51, 399–410.
- Cravens, T.E., Maurelis, A.N., 2001. X-ray emission from scattering and fluorescence of solar x-rays at Venus and Mars. *Geophys. Res. Lett.* 28, 3043–3046.
- Crosby, N.B., Siegmund, O.H.W., Vedder, P.W., Vallerger, J.V., 1993. Extreme Ultraviolet Explorer deep survey observations of a large flare on AU Microscopii. *Astrophys. J. Lett.* 414, L49–L52.
- De Angelis, G., Cloudsley, M.S., Singleterry, R.C., Wilson, J.W., 2004. Mars radiation environment model with visualization. *Adv. Space Res.* 34, 1328–1332.
- Dennerl, K., 2002. Discovery of X-rays from Mars with Chandra. *Astr. Astrophys.* 394, 1119–1128.
- Dion, P., Charbonneau, R., and Thibault, C., 1994. Effect of ionizing dose rate on the radioresistance of some food pathogenic bacteria. *Can. J. Microbiol.* 40, 369–374.
- DiRuggiero, J., Santangelo, N., Nackerdien, Z., Ravel, J., and Robb, F.T., 1997. Repair of extensive ionizing-radiation DNA damage at 95 C in the hyperthermophilic archaeon *Pyrococcus furiosus*. *J. Bacteriology*. 179, 4643–4645.
- Dubrova, Y.E., 2003. Long-term genetic effects of radiation exposure. *Mutation Res.* 544, 433–439.
- Farkas, J., 1998. Irradiation as a method for decontaminating food. *Int. J. Food Microbiology*. 44, 189–204.

- Favata, F., Reale, E., Micela, G., Sciortino, S., Maggio, A., and Matsumoto, H., 2000. An extreme X-ray flare observed on EV Lac by ASCA in July 1998. *Astr. Astrophys.* 353, 987–997.
- Ferreira, A.C., Nobre, M.F., Moore, E., Rainey, F.A., Battista, J.R., da Costa, M.S., 1999. Characterization and radiation resistance of new isolates of *Rubrobacter radiotolerans* and *Rubrobacter xylanophilus*. *Extremophiles*. 3, 235–238.
- Fielden, E.M., and O’Neill, P., 1991. *The Early Effects of Radiation on DNA*. Springer, Berlin.
- Forster, L., Forster, P., Lutz-Bonengel, S., Willkomm, H., and Brinkmann, B., 2002. Natural radioactivity and human mitochondrial DNA mutations. *PNAS* 99, 13950–13954.
- Friedberg, E.C., 2003. DNA damage and repair. *Nature*. 421, 436–440.
- Güdel, M., Audard, M., Kashyap, V.L., Drake, J.J., and Guinan, E.F., 2003. Are coronae of magnetically active stars heated by flares? II. Extreme ultraviolet and X-ray flare statistics and the differential emission measure distribution. *Astrophys. J.* 582, 423–442.
- Gunell, H., Holstrom, M., Kallio, E., Janhunen, P., Dennerl, K., 2004. X rays from solar wind charge exchange at Mars: A comparison of simulations and observations. *Geophys. Res. Lett.* 31, L22801–L22804.
- Haisch, B., Strong, K.T., and Rodono, M.A., 1991. Flares on the sun and other stars. *Ann. Rev. Astr. Astrophys.* 29, 275–324.
- Hawley, S.L. and Pettersen, B.R., 1991. The great flare of 1985 April 12 on AD Leonis. *Astrophys. J.* 378, 725–741.
- Hudson, H.S., 1991. Solar flares, microflares, nanoflares, and coronal heating. *Solar Phys.* 133, 357–369.
- Kanbach, G., Bertsch, D.L., Fichtel, C.E., and 7 others, 1993. Detection of a long-duration solar gamma-ray flare on June 11, 1991 with EGRET on COMPTON-GRO. *Astr. Astrophys. Supp.* 97, 349–353.

- Kopylov, V.M., Bonch-Osmolovskaya, E.A., Svetlichnyi, V.A., Miroshnichenko, M.L., and Skobkin, V.S., 1993. Gamma-irradiation resistance and UV-sensitivity of extremely thermophilic archaeobacteria and eubacteria. *Mikrobiologiya*. 62, 90–95.
- Krucker, S., and Lin, R.P., 2002. Relative timing and spectra of solar flare hard X-ray sources. *Solar Phys*. 210, 229–243.
- Lee, T.T., Petrosian, V., and McTiernan, J.M., 1993. The distribution of flare parameters and implications for coronal heating. *Astrophys. J.* 412, 401–409.
- Liebert, J., Kirkpatrick, J.D., Reid, I.N., and Fisher, M.D., 1999. A 2MASS ultra-cool M dwarf observed in a spectacular flare. *Astrophys. J.* 519, 345–353.
- Lin, R.P., Feffer, P.T., Schwartz, R.A., 2001. Solar hard X-ray bursts and electron acceleration down to 8 keV. *Astrophys. J. Lett.* 557, L125–L128.
- Mancinelli, R.L., and Klovstad, M., 2000. Martian soil and UV radiation: microbial viability assessment on spacecraft surfaces. *Plan. Sp. Sci.* 48, 1093–1097.
- Mileikowsky, C., Cucinotta, F.A., Wilson, J.W., and 7 others, 2000. Natural transfer of viable microbes in space. 1. From Mars to Earth and Earth to Mars. *Icarus*. 145, 391–427.
- Molina-Cuberos, G.J., Stumptner, W., Lammer, H., Komle, N.I., O'Brian, K., 2001. Cosmic ray and UV radiation models on the ancient martian surface. *Icarus*. 154, 216–222.
- Pagano, I., Ventura, R., Rodono, M., Peres, G., and Micela, G., 1997. A major optical flare on the recently discovered X-ray active dMe star G 102-21. *Astr. Astrophys.* 318, 467–471.
- Pavlov, A.K., Blinov, A.V., Konstantinov, A.N., 2002. Sterilization of Martian surface by cosmic radiation. *Plan. Sp. Sci.* 50, 669–673.
- Qiu, J., Liu, C., Gary, D.E., Nita, G.M., Wang, H., 2004. Hard X-ray and microwave observations of microflares. *Astrophys. J.* 612, 530–545.
- Quillardet, P., Rouffaud, M.A., and Bouige, P., 2003. DNA array analysis of gene

expression in response to UV irradiation in *Escherichia Coli*. Res. Microbiol. 154, 559–572.

Randall, C.E., Harvey, V.L., and 9 others, 2005. Stratospheric effects Of energetic particle precipitation in 2003–2004. Geophys. Res. Lett. 32, L05802–L05805.

Reedy, R.C., Arnold, J.R., Lal, D., 1983. Cosmic-ray record in solar system matter. Science. 219, 127–135.

Rohwer, R.G., 1984. Scrapie infectious agent is virus-like in size and susceptibility to inactivation. Nature. 308, 658–662.

Ross, A.J., Webbon, B., Simonsen, L.C., Wilson, J.W., 1997. Shielding strategies for human space exploration. Wilson, J.W., Miller, J., Konradi, A., Cucinotta, F.A. (eds.). NASA CP 3360, 283–296.

Rubenstein, E.P., and Schaefer, B.E., 2000. Are superflares on solar analogues caused by extrasolar planets? Astrophys. J.. 529, 1031–1033.

Russell, A.D., 1982. The destruction of bacterial spores. Academic Press, New York.

Ryan, J.M., 2000. Long-duration solar gamma-ray flares. Sp. Sci. Rev. 93, 581–610.

Saganti, P.B., Cucinotta, F.A., Wilson, J.W., Simonsen, L.C., Zeitlin, C., 2004. Radiation climate map for analyzing risks to astronauts on the Mars surface from galactic cosmic rays. Sp. Sci. Rev. 110, 143–156.

Sankaranarayanan, K., 1982. Genetic Effects of Ionizing Radiation in Multicellular Eukaryotes and the Assessment of Genetic Radiation Hazards in Man. Elsevier Biomedical, Amsterdam.

Sankaranarayanan, K., Chakraborty, R., 2000. Ionizing radiation and genetic risks. XI. The doubling dose estimates from the mid-1950s to present and the conceptual change to the use of human data on spontaneous mutation rates and mouse data on induced mutation rates for doubling dose calculations. Mutat. Res. 453, 107–127.

Schaefer, B.E., King, J.R., Deliyannis, C.P., 2000. Superflares on ordinary solar-

type stars. *Astrophys. J.* 529, 1026–1030.

Schimmerling, W., Wilson, J.W., Nealy, J.E., Thibeault, S.A., Cucinotta, F.A., Shinn, J.L., Kim, M., Kiefer, R., 1996. Shielding against Galactic cosmic rays. *Adv. Sp. Res.* 17, (2)31–(2)36.

Schuerger, A.C., Mancinelli, R.L., Kern, R.G., Rothschild, L.J., McKay, C.P., 2003. Survival of endospores of *Bacillus subtilis* on spacecraft surfaces under simulated martian environments: Implications for the forward contamination of Mars. *Icarus.* 165, 253–276.

Setlow, R.B., Pollard, E.C. 1962. *Molecular Biophysics.* Addison-Wesley, Reading, MA.

Smith, D.S., Scalo, J., Wheeler, J.C., 2004a. Importance of biologically active aurora-like UV emission: Stochastic irradiation of Earth and Mars by flares and explosions. *Origins Life Evol. Biosphere.* 34, 513–532.

Smith, D.S., Scalo, J., Wheeler, J.C., 2004b. Transport of ionizing radiation in terrestrial-like exoplanet atmospheres. *Icarus.* 171, 229–253.

Sparrow, A.H., Underbrink, A.G., Sparrow, R.C., 1967. Chromosomes and cellular radiosensitivity. I. The relationship of D<sub>0</sub> to chromosome volume and complexity in seventy-nine different organisms. *Rad. Res.* 31, 915–949.

Sparrow, A.H., Underbrink, A.G., Rossi, H.H., 1972. Mutations induced in *Tradescantia* by small doses of X-rays and neutrons: analysis of dose-response curves. *Science.* 176, 916–918.

Stothers, R., 1980. Giant solar flares in Antarctic ice. *Nature.* 287, 365–365.

Sutherland, B.M., Bennett, P.V., Sidorkina, O., Laval, J., 2000. Clustered DNA damages induced in isolated DNA in human cells by low doses of ionizing radiation. *Proc. Natl. Acad. Sci.* 97, 103–108.

Turner, J.E., 1995. *Atoms, Radiation, and Radiation Protection.* Wiley, New York.

UNSCEAR 2001. *Hereditary Effects of Radiation.* United Nations, New York.

Veronig, A., Temmer, M., Hanslmeier, A., Otruba, W., Messerotti, M., 2002. Tem-

poral aspects and frequency distributions of solar soft X-ray flares. *Astr. Astrophys.* 382, 1010–1080.

Violot, D., M'kacher, R., Adjadj, E., Dossou, J., de Vathaire, F., Parmentier, C., 2005. Evidence of increased chromosomal abnormalities in French Polynesian thyroid cancer patients. *Eur. J. Nucl. Med. Mol. Imaging.* 32, 174–179.

von Sonntag, C., 1987. *The chemical basis of radiation biology.* Taylor and Francis, London.

Wänke, H., Brückner, J., Dreibus, G., Rieder, R., Ryabchikov, I., 2001. Chemical composition of rocks and soils at the Pathfinder site. *Sp. Sci. Rev.* 96, 317–330.

Ward, J.F., 1999. Ionizing radiation damage to DNA: A challenge to repair systems. In: Dizdaroglu, M., Karakaya, A.E. (Eds.), *Advances in DNA damage and repair: Oxygen radical effects, cellular protection, and biological consequences.* Kluwer/Plenum, NY, pp. 431–439.

Wilson, J.W., Cucinotta, F.A., Kim, M.-H.Y., Schimmerling, W., 2001. Optimized shielding for space radiation protection. *Physica Medica.* XVII, 67–71.

Woods, T.N., Eparvier, F.G., Fontenla, J., Harder, J., Kopp, G., McClintock, W.E., Rottman, G., Smiley, B., and Snow, M., 2004. Solar irradiance variability during the October 2003 solar storm period. *Geophys. Res. Lett.* 31, L10802–10806.